

Article scientifique

Article

2008

Accepted version

Open Access

This is an author manuscript post-peer-reviewing (accepted version) of the original publication. The layout of the published version may differ .

---

## Robust and efficient quantum repeaters with atomic ensembles and linear optics

---

Sangouard, Nicolas; Simon, Christoph; Zhao, Bo; Chen, Yu-Ao; de Riedmatten, Hugues; Pan, Jian-Wei; Gisin, Nicolas

### How to cite

SANGOUARD, Nicolas et al. Robust and efficient quantum repeaters with atomic ensembles and linear optics. In: Physical review, A, Atomic, molecular, and optical physics, 2008, vol. 77, n° 062301, p. 1–7. doi: 10.1103/PhysRevA.77.062301

This publication URL: <https://archive-ouverte.unige.ch/unige:886>

Publication DOI: [10.1103/PhysRevA.77.062301](https://doi.org/10.1103/PhysRevA.77.062301)

# Robust and Efficient Quantum Repeaters with Atomic Ensembles and Linear Optics

Nicolas Sangouard,<sup>1</sup> Christoph Simon,<sup>2</sup> Bo Zhao,<sup>3</sup> Yu-Ao Chen,<sup>3</sup>

Hugues de Riedmatten,<sup>2</sup> Jian-Wei Pan<sup>3</sup>, and Nicolas Gisin<sup>2</sup>

<sup>1</sup>*Laboratoire MPQ, UMR CNRS 7162, Université Paris 7, France*

<sup>2</sup>*Group of Applied Physics, University of Geneva, Switzerland*

<sup>3</sup>*Physikalisches Institut, Universität Heidelberg, Germany*

(Dated: May 13, 2008)

In the last few years there has been a lot of interest in quantum repeater protocols using only atomic ensembles and linear optics. Here we show that the local generation of high-fidelity entangled pairs of atomic excitations, in combination with the use of two-photon detections for long-distance entanglement generation, permits the implementation of a very attractive quantum repeater protocol. Such a repeater is robust with respect to phase fluctuations in the transmission channels, and at the same time achieves higher entanglement generation rates than other protocols using the same ingredients. We propose an efficient method of generating high-fidelity entangled pairs locally, based on the partial readout of the ensemble-based memories. We also discuss the experimental implementation of the proposed protocol.

PACS numbers: 03.67.Hk, 03.67.Mn, 42.50.Md, 76.30.Kg

## I. INTRODUCTION

The distribution of entangled states over long distances is difficult because of unavoidable transmission losses and the no-cloning theorem for quantum states. One possible solution is the use of quantum repeaters [1]. In this approach, entanglement is generated independently for relatively short elementary links and stored in quantum memories. Entanglement over longer distances can then be created by entanglement swapping.

The Duan-Lukin-Cirac-Zoller (DLCZ) protocol [2] relies on Raman scattering in atomic ensembles, which can create a single “Stokes” photon correlated with a collective atomic excitation. Two remote atomic ensembles can then be entangled based on the detection at a central station of a single Stokes photon, which could have been emitted by either of the two ensembles [3]. The entanglement can then be extended to long distances by converting back the atomic excitations into “Anti-Stokes” photons via the reverse Raman process and performing successive entanglement swapping operations, which are also based on the detection of a single Anti-Stokes photon.

The DLCZ protocol is attractive because it uses relatively simple ingredients. Over the last few years there has been a lot of experimental activity towards its realization [4], including the creation of entanglement between separate quantum nodes [5] and the realization of teleportation between photonic and atomic qubits [6]. Conversion efficiencies from atomic to photonic excitations as high as 84 percent have recently been achieved for ensembles inside optical cavities [7].

However the DLCZ protocol also has a certain number of practical drawbacks. On the one hand, the *generation* of entanglement via single-photon detections requires interferometric stability over the whole distance, which *a priori* seems quite challenging. For recent experimental work towards assessing the feasibility of this requirement

for optical fiber links see Ref. [8].

On the other hand, the *swapping* of entanglement using single-photon detections leads to the growth of a vacuum component in the generated state, and to the rapid (quadratic with the number of links) growth of errors due to multiple emissions from individual ensembles. In order to suppress these errors, one then has to work with very low emission probabilities. These factors together lead to rather low entanglement distribution rates for the DLCZ protocol. See Fig. 1, curve B, for its performance in the distance range from 400 km to 1200 km. Moreover, the DLCZ protocol does not contain a procedure for entanglement purification (of phase errors in particular), which limits the total number of links that can be used.

This paper is organized as follows. In section II we compare the entanglement generation times for the DLCZ protocol and for a number of recently proposed improved protocols that use the same ingredients [9, 10, 11, 12]. We show that an approach that combines the *local generation of high-fidelity entangled pairs of atomic excitations* and the creation and swapping of long-distance entanglement via *two-photon detections* is particularly promising in terms of robustness and achievable entanglement generation rate. The main drawback of the implementation of this approach proposed in Ref. [10] is its relatively high complexity for local pair generation, which also has a negative impact on the fidelity of the created pairs for non-unit memory and detection efficiency. In section III we propose an improved method for the local generation of entangled pairs of atomic excitations based on the *partial readout* of the atomic ensemble memories. In section IV we calculate the entanglement generation times for a quantum repeater using this new source of pairs. The resulting protocol is both robust with respect to phase fluctuations in the transmission channels and significantly more efficient than all other protocols (known to us) that use the same ingredients. In section V we discuss the prospects of experimental implementa-

tion.

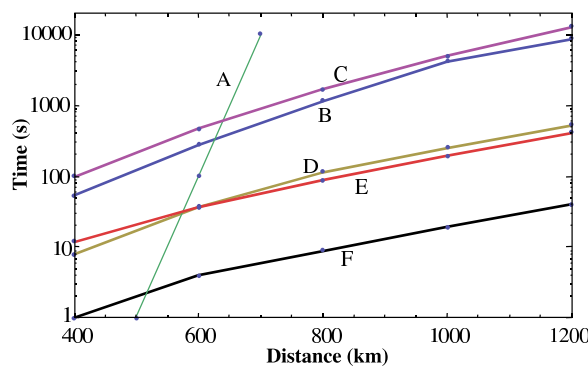


FIG. 1: (Color online) Comparison of different quantum repeater protocols that all use only atomic ensembles and linear optics. The quantity shown is the average time needed to distribute a single entangled pair for the given distance. A: as a reference, the time required using direct transmission of photons through optical fibers, with losses of 0.2 dB/km, corresponding to the best available telecom fibers at a wavelength of  $1.5 \mu\text{m}$ , and a pair generation rate of 10 GHz. B: the original DLCZ protocol that uses single-photon detections for both entanglement generation and swapping [2]. C: the protocol of Ref. [10] section III.B which first creates entanglement locally using single-photon detections, and then generates long-distance entanglement using two-photon detections. D: protocol of Ref. [11] that uses quasi-ideal single photon sources (which can be implemented with atomic ensembles, cf. text) plus single-photon detections for generation and swapping. E: protocol of Ref. [10] section III.C that locally generates high-fidelity entangled pairs and uses two-photon detections for entanglement generation and swapping. F: the proposed new protocol which follows the approach of Ref. [10] section III.C, but uses an improved method of generating the local entanglement. The performance of the protocol of Ref. [9] is close to curve B for this distance range (the authors announce a factor of 2 improvement over DLCZ at 640 km and a factor of 5 at 1280 km). For all the curves we have assumed memory and detector efficiencies of 90%. The numbers of links in the repeater chain are optimized for curves B and D, e.g. giving 4 links for 600 km and 8 links for 1000 km for both protocols. For curves C, E and F, we imposed a maximum number of 16 links (cf. text), which is used for all distances for curve C and for distances greater than 400 km for curves E and F.

## II. MODIFICATIONS OF THE DLCZ PROTOCOL - COMPARISON

Ref. [9] recently proposed a modification of the DLCZ protocol in which entanglement is still generated by single-photon detections, but entanglement swapping is based on two-photon detections. As a consequence, the vacuum component remains constant under entanglement swapping, multi-photon errors grow only linearly,

Reference	generation	swapping	resources	links	time
[2]	1	1	4	8	B
[9]	1	2	4	16	-
[10] III.B	2	2	8	16	C
[11]	1	1	4	8	D
[12]	2	2	4	16	-
[10] III.C	2	2	12	16	E
new	2	2	8	16	F

TABLE I: Characteristics of the main protocols for quantum repeaters based on atomic ensembles. Column 1 gives the reference for the considered protocol. Columns 2 and 3 show the number of photons detected in the long-distance entanglement generation step and in the subsequent entanglement swapping steps respectively. Column 4 gives the number of atomic ensembles used within each elementary link. Column 5 gives the number of links for a distance of 1000 km. The number of links is optimized for protocols [2, 11] and limited to 16 for the other protocols, cf. text. For the protocol of ref. [9], we have taken the number of links announced by the authors for a distance of 640km. The last column refers to the curves of Fig. 1, where the performance of the protocols is compared.

and entanglement purification with linear optics [13] is possible. However the achieved rates are only slightly better than for the DLCZ protocol for distances of order 1000 km (see also caption of Fig. 1), mainly because errors in the elementary link due to multiple excitations still force one to work with low emission probabilities. Multiple excitations are hard to detect in the entanglement generation process because the corresponding Stokes photons have to propagate far and are lost with high probability.

In Ref. [10], several protocols based on two-photon detections were presented. The one presented in section III.B is a simple variation of the proposal of Ref. [9], in which the entanglement generation step of Ref. [9] is performed locally and the first entanglement swapping step of Ref. [9] is performed remotely. This protocol does not require interferometric stability over long distances. However, excess photon emissions in the remote swapping step remain undetected due to fiber losses. As a consequence, the distributed state after the remote swapping has large vacuum and single-photon components, which lead to small success probabilities for the subsequent swapping steps, and thus to a rather low overall entanglement distribution rate, comparable to the DLCZ protocol (see curve C in Fig.1).

Ref. [11] uses single-photon detections for entanglement generation and swapping, but the method of entanglement generation is different with respect to the DLCZ protocol, relying on single-photon sources. This makes it possible to improve the distribution rate of entangled states, thanks to the suppression of multi-photon errors. This protocol can be realized with atomic ensembles and

linear optics because a quasi-ideal single-photon source can be constructed based on atomic ensembles of the DLCZ type [14]. The probabilistic emission of the Stokes photon heralds the creation of an atomic excitation in the ensemble. The charged memory can now be used as a single-photon source by reconverting the stored excitation into an Anti-Stokes photon. The probability for this source to emit two Anti-Stokes photons can be made arbitrarily small by working with a small emission probability for the Stokes photon. The price to pay is that the preparation of the source requires many attempts until the Stokes photon is emitted. However, these attempts are purely local and can thus be repeated very fast. The protocol of Ref. [11] is faster than the DLCZ protocol, see curve D in Fig. 1. However it shares the need for phase stability, the amplification of vacuum and multi-photon components, and the absence of a known entanglement purification procedure.

Ref. [12] proposed a scheme in which both entanglement creation and swapping are based on two-photon detections [15]. In addition to the advantages mentioned for Ref. [9], this protocol no longer requires interferometric stability over long distances. However, in the scheme of Ref. [12], entanglement is directly generated over long distances. Since only a small excitation probability can be used for each entanglement generation attempt (in order to avoid multi-photon errors), and since after every attempt one has to communicate its success or failure over a long distance, the required entanglement generation time becomes longer than for the DLCZ protocol.

Ref. [10] proposed a number of protocols without making a quantitative comparison. We have found that the best performing of these protocols is the one presented in section III.C of Ref. [10]. In this approach one first locally generates high-fidelity entangled pairs of atomic excitations that are stored in nearby ensembles. Then long-distance entanglement is generated and swapped via two-photon detections. We have calculated the entanglement generation times for this protocol. Its performance is shown as curve E in Fig. 1. One can see that the entanglement distribution time is comparable with the protocol of Ref. [11]. Since high-fidelity pairs are first generated locally, the effective “excitation probability” for every long-distance entanglement generation attempt is essentially equal to one. Moreover, the vacuum component remains unchanged under entanglement swapping thanks to the use of two-photon detections, leading to high success probabilities for the higher-order swapping operations. To fully profit from this scheme, the local pair generation rate has to be sufficiently high, cf. below.

The use of two-photon detections for long-distance entanglement generation makes the scheme robust with respect to phase fluctuations in the channels, but also more sensitive to photon losses than the schemes that use single-photon detections for the same purpose [2, 9, 11]. As a consequence, the two-photon protocol favors larger numbers of elementary links for the same distance com-

pared to the single-photon schemes. In fact, the optimal number of links for 1000 km, e.g., would be 32. In Fig. 1, we have limited the maximum number of links used to 16, to keep it more comparable to the link numbers for the single-photon schemes, and to have link numbers for which it is plausible that entanglement purification may not be necessary. Note however that the scheme is perfectly compatible with the use of linear optics entanglement purification as proposed in Ref. [13], whereas no entanglement purification protocol is currently known for the schemes of Refs. [2, 11]. Furthermore the stability requirements are much more stringent for the single-photon schemes, so achieving sufficiently low error rates for a single-photon based quantum repeater with 8 links is likely to be more difficult than for a two-photon based quantum repeater with 16 links. Our comparison method is thus quite conservative concerning the advantage of the two-photon protocol.

A related important question is that of complexity, in particular the number of atomic ensembles required for a given repeater, compared to the achieved improvement in the entanglement generation time, see also Table I. The schemes of Refs. [2, 9, 11] require just four ensembles per elementary link [16]. The scheme of Ref. [10] section III.C requires twelve, since every local pair generation uses four single-photon sources (which can be realized with ensembles as described above) and two EIT-based ensemble memories [17]. Together with the increased number of links discussed above, this means that this protocol is much less efficient than that of Ref. [11]. It should be noted however that the two-photon protocol [10] section III.C still remains much more robust with respect to channel phase fluctuations than the single-photon protocol [11].

In the following we propose a new method for the local generation of high-fidelity entangled pairs of atomic excitations. The method uses the available resources (atomic ensembles) more efficiently, which makes it possible to achieve *higher-fidelity* entanglement for the same values of memory and detection efficiency, leading to a significant improvement in the achievable entanglement generation rate over long distances. The performance of the improved protocol is shown as curve F in Fig. 1. For the new protocol, which requires eight memories per elementary link, the gain in time clearly outweighs the modest increase in complexity compared to the fastest single-photon protocol [11]. For example, for 1000 km the new protocol uses four times as many memories, but it is about 13 times faster. (The rate improvement compared to the DLCZ protocol, which uses the same number of memories as Ref. [11], is by a factor of 200.) It is thus not only robust, but also the most efficient repeater protocol known to us for the given ingredients.

### III. LOCAL GENERATION OF HIGH-FIDELITY ENTANGLED PAIRS BASED ON PARTIAL MEMORY READOUT

Ref. [10] proposed to generate high-fidelity entangled pairs of atomic excitations locally by using four single-photon sources (which can be realized with DLCZ-type ensembles, cf. above), linear optical elements, and two EIT-based quantum memories, cf. Fig. 11 of Ref. [10]. Four photons are emitted by the ensembles serving as sources, two of them are detected, two are absorbed again by the EIT memories. This double use of the memories (emission followed by storage) leads to relatively large errors (vacuum and single-photon contributions) in the created state if the memory efficiencies are smaller than one. These errors then have a negative impact on the success probabilities of the entanglement generation and swapping operations, and thus on the overall time needed for long-distance entanglement distribution.

Here we propose a different method for the local generation of high-fidelity entangled pairs of atomic excitations, which is based on the *partial readout* of ensemble memories. Our scheme does not use any emission followed by storage. For the same memory and detection efficiency, it leads to higher quality entangled pairs compared to the method of Ref. [10], and as a consequence to a significantly improved rate for the overall quantum repeater protocol (curve E in Fig. 1). We now describe the proposed method for local entanglement generation in detail.

The proposed setup uses four atomic ensembles. Atomic Raman transitions are coherently excited such that a Stokes photon can be emitted with a small probability  $p$ . This Stokes photon has a well defined polarization : the horizontally (vertically) polarized modes are labeled by  $a_h^\dagger$  and  $b_h^\dagger$ , ( $a_v^\dagger$  and  $b_v^\dagger$ ) and are produced from upper (lower) atomic ensembles  $A_h$  and  $B_h$  ( $A_v$  and  $B_v$ ) as represented in Fig. 2. The four atomic ensembles are repeatedly excited *independently* with a repetition rate  $r$  until a Stokes photon has been detected in each mode  $a_h^\dagger$ ,  $a_v^\dagger$ ,  $b_h^\dagger$ , and  $b_v^\dagger$ . The detection of a Stokes photon heralds the storage of a single atomic spin excitation in each ensemble, labeled by  $s_{ah}^\dagger$ ,  $s_{av}^\dagger$ ,  $s_{bh}^\dagger$  or  $s_{bv}^\dagger$  depending on the location. The average waiting time for successful charging of all four ensembles is approximately given by  $T = \frac{1}{rp}(\frac{1}{4} + \frac{1}{3} + \frac{1}{2} + 1) = \frac{25}{12rp}$ . Thanks to the independent creation and storage, it scales only like  $1/p$ . Once all ensembles are charged, the four stored spin-wave modes are then *partially* converted back into a photonic excitations. This is done using read pulses whose area is smaller than the standard value of  $\pi$ , such that the state of the system is given by  $(\alpha a_h'^\dagger + \beta s_{ah}^\dagger) \otimes (\alpha a_v'^\dagger + \beta s_{av}^\dagger) \otimes (\alpha b_h'^\dagger + \beta s_{bh}^\dagger) \otimes (\alpha b_v'^\dagger + \beta s_{bv}^\dagger) |0\rangle$  with  $|\alpha|^2 + |\beta|^2 = 1$ . The primed modes  $a_h'^\dagger$ ,  $a_v'^\dagger$ , ( $b_h'^\dagger$ ,  $b_v'^\dagger$ ) refer to the emitted Anti-Stokes photons from memories located at  $A_h$  and  $A_v$  ( $B_h$  and  $B_v$ ) respectively;  $|0\rangle$  denotes the empty state. The released Anti-Stokes photons are combined at a central station

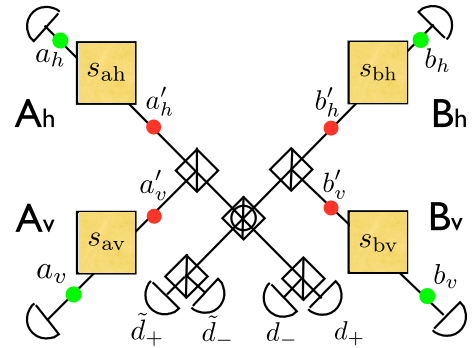


FIG. 2: (Color online) Setup for generating high-fidelity entangled pairs of atomic excitations. Yellow squares represent atomic ensembles which probabilistically emit Stokes photons (green dots). The conditional detection of a single Stokes photon heralds the storage of one atomic spin-wave excitation. In this way an atomic excitation is created and stored independently in each ensemble. Then all four ensembles are simultaneously read out *partially*, creating a probability amplitude to emit an Anti-Stokes photon (red dots). The coincident detection of two photons in  $d_+$  and  $\tilde{d}_+$  projects non-destructively the atomic cells into the entangled state  $|\Phi_{ab}\rangle$  of Eq. (1);  $d_+ - \tilde{d}_-$ ,  $d_- - \tilde{d}_+$ , and  $d_- - \tilde{d}_-$  coincidences, combined with the appropriate one-qubit transformations, also collapse the state of the atomic cells into  $|\Phi_{ab}\rangle$ . Half-circles represent photon detectors. Vertical bars within squares label polarizing beam splitters (PBS) that transmit (reflect)  $H$  ( $V$ )-polarized photons. The central PBS with a circle performs the same action in the  $\pm 45^\circ$  ( $H + V/H - V$ ) basis.

where they are detected in modes  $d_{\pm} = a'_h + a'_v \pm b'_h \mp b'_v$  and  $\tilde{d}_{\pm} = \pm a'_h \mp a'_v + b'_h + b'_v$ , using the setup shown in Fig. 2. In the ideal case, a twofold coincident detection between  $d_+$  and  $\tilde{d}_+$  projects the state of the two remaining spin-wave modes non-destructively onto

$$|\Phi_{ab}\rangle = 1/\sqrt{2}(s_{ah}^\dagger s_{bh}^\dagger + s_{av}^\dagger s_{bv}^\dagger)|0\rangle. \quad (1)$$

The stored atomic excitations can be reconverted into photons as desired. In the proposed quantum repeater protocol (cf. sec. IV), one excitation (e.g. the one in the  $B$  ensembles) is reconverted into a photon right away and used for entanglement generation. The other excitation is reconverted later for entanglement swapping or for the final use of the entanglement. Note that the setup can also be used as a heralded source of single photon pairs [18, 19].

Given an initial state where all four memories are charged, the probability for a coincidence between  $d_+$  and  $\tilde{d}_+$  is given by  $\frac{1}{2}\alpha^4\beta^4$ . Since the twofold coincidences  $d_+ - \tilde{d}_-$ ,  $d_- - \tilde{d}_+$ ,  $d_- - \tilde{d}_-$  combined with the appropriate one-qubit transformation also collapse the state of the atomic ensembles into  $|\Phi_{ab}\rangle$ , the overall success probability for the entangled pair preparation is given by  $P_s = 2\alpha^4\beta^4$ .

We now analyze the effect of non-unit detector effi-

ciency  $\eta_d$  and memory recall efficiency  $\eta_m$ . The waiting time for the memories to be charged is now  $T^\eta = T/\eta_d = \frac{25}{12r_{pd}}$ . Furthermore, the detectors can now give the expected coincidences when three or four Anti-Stokes photons are released by the memories, but only two are detected. In this case, the created state contains additional terms including single spin-wave modes and a vacuum component,

$$\begin{aligned} \rho_{ab}^s = & c_2^s |\Phi_{ab}\rangle\langle\Phi_{ab}| \\ & + c_1^s (|s_{ah}\rangle\langle s_{ah}| + |s_{av}\rangle\langle s_{av}| + |s_{bh}\rangle\langle s_{bh}| + |s_{bv}\rangle\langle s_{bv}|) \\ & + c_0^s |0\rangle\langle 0|; \end{aligned} \quad (2)$$

where  $c_2^s = 2\alpha^4\beta^4\eta^2/P_s^\eta$ ,  $c_1^s = \alpha^6\beta^2\eta^2(1-\eta)/P_s^\eta$  and  $c_0^s = 2\alpha^8(1-\eta)^2\eta^2/P_s^\eta$ . Here  $\eta = \eta_m\eta_d$  is the product of the memory recall efficiency and the (photon-number resolving) detector efficiency, and we have introduced a superscript  $s$  for ‘‘source’’. The probability for the successful preparation of this mixed state is  $P_s^\eta = 2\eta^2\alpha^4(1-\alpha^2\eta)^2$ . The fidelity of the conditionally prepared state is equal to the two-photon component  $c_2^s = \beta^4/(1-\alpha^2\eta)^2$ . As can be seen from the two previous equations, there is a tradeoff on the readout coefficients  $\alpha, \beta$ . The creation of an entangled state with a high fidelity favors  $\alpha \approx 0$ , whereas a high success probability favors  $\alpha \approx \beta \approx 1/\sqrt{2}$ .

#### IV. REPEATER PROTOCOL

We now include our source of heralded pairs within a quantum repeater protocol following Ref. [10]. Fig. 3A shows how entanglement between two remote sources (denoted AB and CD) is created by combining two Anti-Stokes photons at a central station, where one photon is released from the B ensembles and the other from the C ensembles, and performing a projective measurement into the modes  $D_{\pm}^{bc} = b_h' \pm c_v'$  and  $D_{\pm}^{cb} = c_h' \pm b_v'$  using the same combination of linear optical elements as in Refs. [9, 10, 12]. The twofold coincident detection  $D_+^{bc}-D_-^{cb}$  ( $D_+^{bc}-D_-^{cb}$ ,  $D_-^{bc}-D_+^{cb}$ , or  $D_-^{bc}-D_-^{cb}$  combined with the appropriate one-qubit operations) collapses the two remaining full memories into  $|\Phi_{ad}\rangle$ . Due to imperfections, the distributed state  $\rho_{ad}^0$  includes vacuum and single spin-wave modes. One can show that their weights  $c_2^0, c_1^0, c_0^0$  are unchanged compared with the weights of the source state  $\rho_{ab}^s$ , because  $c_2^0 = \frac{(c_2^s)^2}{(c_2^s+2c_1^s)^2} = c_2^s$ ,  $c_1^0 = \frac{c_1^s c_2^s}{(c_2^s+2c_1^s)^2} = c_1^s$  and  $c_0^0 = \frac{4(c_2^s)^2}{(c_2^s+2c_1^s)^2} = c_0^s$ . (The condition for having a stationary state is  $c_0 c_2 = 4(c_1)^2$ , which is fulfilled by  $c_2^s, c_1^s, c_0^s$ .) The success probability for the entanglement creation is given by  $P_0 = 2\eta^2\eta_t^2(c_2^s/2 + c_1^s)^2$ . Here  $\eta_t$  is the fiber transmission for each photon.

Fig. 3B shows how, using the same combination of linear optical elements and detectors, one can perform successive entanglement swapping operations, such that the state  $\rho_{az}^n$  is distributed between the distant locations

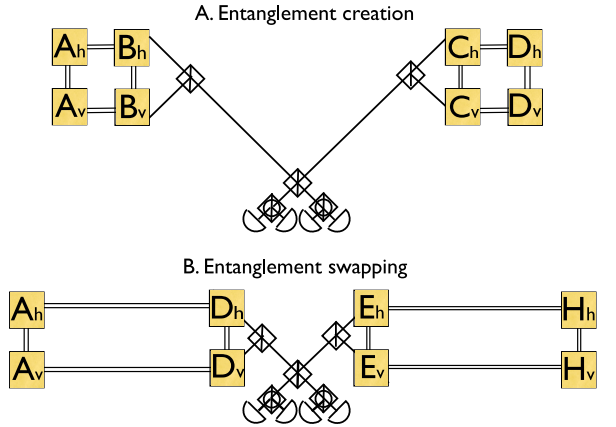


FIG. 3: (Color online) (A) Long-distance entanglement creation using two four-ensemble sources as shown in Fig. 2. The A and D ensembles are entangled by the detection of two photons emitted from the B and C ensembles, using the same setup as in Refs. [9, 10, 12]. Note that the AB source is separated from the CD source by a long distance. (B) Entanglement swapping. The same set of linear optical elements allows one to entangle the A and H ensembles belonging to two adjacent elementary links. Note that the D and E ensembles are at the same location.

A and Z after  $n$  swapping operations. In analogy to above, one can show that the distributed state  $\rho_{az}^n$  includes vacuum and single spin-wave components with unchanged weights with respect to the initial ones, i.e.  $c_2^n = c_2^s$ ,  $c_1^n = c_1^s$  and  $c_0^n = c_0^s$ . From the expression of  $P_0$  and keeping in mind that the entanglement swapping operations are performed locally such that there are no transmission losses, one deduces the success probability for the  $i$ -th swapping,  $P_i = 2\eta^2(c_2^s/2 + c_1^s)^2$ . The two-spin-wave component of the distributed mixed state  $|\Phi_{az}\rangle$  is finally post-selected with the probability  $P_{\text{pr}} = c_2^s\eta^2$ .

The time required for a successful distribution of an entangled state  $|\Phi_{az}\rangle$  is approximately given by [20]

$$T_{\text{tot}} = \left(\frac{3}{2}\right)^n \frac{L_0}{c} \frac{1}{P_0 P_1 \dots P_n P_{\text{pr}}}, \quad (3)$$

where  $L_0 = L/2^n$  is the length of an elementary link,  $L$  is the total distance and  $n$  is the nesting level of the repeater. Taking into account the expressions of  $P_0$ ,  $P_i$  (with  $i \geq 1$ ) and  $P_{\text{pr}}$ , one can rewrite  $T_{\text{tot}}$  as

$$T_{\text{tot}} = 2 \times 3^n \times \frac{L_0}{c} \frac{(1-\alpha^2\eta)^{2(n+2)}}{\eta_t^2\eta^{2(n+2)}\beta^{4(n+2)}}. \quad (4)$$

Here  $\eta_t = e^{-L_0/(2L_{\text{att}})}$  is the fiber transmission, with the attenuation length  $L_{\text{att}}$ . In our numerical examples we use  $L_{\text{att}} = 22$  km, corresponding to losses of 0.2 dB/km, which are currently achievable at a wavelength of 1.5  $\mu\text{m}$  [21];  $c = 2 \times 10^8$  m/s is the photon velocity in the fiber.

For these formulas to be strictly valid, the source preparation time has to be negligible compared to the communication time, i.e. in our case  $T_s = \frac{3T\eta}{2P_s} \ll \frac{L_0}{c}$ . Otherwise one simply has to replace  $\frac{L_0}{c}$  by  $\frac{L_0}{c} + T_s$ , cf. below.

We now consider the role of errors due to the creation of two excitations in a single memory. Note that in the local entanglement generation process of Fig. 2 a large part of such multi-photon events will be detected because both Stokes and Anti-Stokes photons are detected locally and thus potentially with high efficiency. We find by explicit calculation that the fidelity of the distributed state at the first order in  $p$  after  $n = 4$  swapping levels (neglecting other errors) is given by

$$F \approx 1 - [(418 - 260\eta) + (47 - 205\eta)\alpha^2] (1 - \eta_d)p.$$

If one wants a fidelity of the final state  $F = 0.9$ , one can choose e.g.  $\alpha^2 = 0.2$  and  $p = 6 \times 10^{-3}$ . This is the value of  $\alpha$  used in Fig. 1. For these values, equality between the source preparation time  $T_s$  and the communication time  $L_0/c$  (e.g. for  $L = 1000$  km and 16 links) is reached for a basic repetition rate  $r$  of order 60 MHz, cf. below.

## V. IMPLEMENTATION

In this section we discuss potential experimental implementations of the proposed protocol. There has recently been impressive progress on the efficiency of conversion from atomic excitation to photon, which sets the fundamental limit for the memory efficiency. Values as high as 84 percent have been achieved with a cavity setup [7].

Current DLCZ-type experimental setups with atomic gases [4, 5, 6] are very well suited for demonstrating the proposed ideas. Current repetition rates  $r$  in DLCZ-type experiments are of order a few MHz. To fully exploit the potential of the proposed protocol, the rates have to be increased, cf. above. Rates of tens of MHz, which could already bring the overall entanglement generation times to within a factor of 2 or 3 of the values given in Fig. 1, are compatible with typical atomic lifetimes. With atomic gases, further improvements in  $r$  could be achieved using the Purcell effect in high-finesse cavities to reduce the atomic lifetimes.

Ref. [20] pointed out that the combination of a photon pair source and of a quantum memory which stores one of the photons is equivalent to a DLCZ-type atomic ensemble, which emits a photon that is correlated with an atomic excitation. This approach may make it possible to achieve even higher values of  $r$ , using e.g. photon pair sources based on parametric down-conversion and solid-state quantum memories based on controlled reversible inhomogeneous broadening [22]. Solid-state atomic ensembles, e.g. rare-earth ion doped crystals, furthermore hold the promise of allowing very long storage times (which are essential for quantum repeaters), since the storage time is no longer limited by atomic motion,

while the intrinsic atomic coherence times can be very high. For example, hyperfine coherence times as long as 30 s have been demonstrated in  $\text{Pr:Y}_2\text{SiO}_5$  [23]. The best efficiency published so far for a CRIB memory (in the same material) is 15 % [24], but experiments are progressing quite rapidly. This approach furthermore holds the promise of allowing temporal multiplexing [20], leading to a potential further improvement in the entanglement creation rate, provided that multi-mode memories with the required characteristics can be realized. The main requirements are sufficient optical depth and sufficient memory bandwidth. Other forms of multiplexing could also be possible and might allow to relax the requirements on the memory storage times [25]. Ideally the memories in the described protocol should operate at the optimal wavelength for telecom fibers, i.e. at  $1.5 \mu\text{m}$ . This may be possible with Erbium-doped crystals [26]. Alternatively, wavelength conversion techniques could be employed [27].

Good photon detectors with photon number resolution are also essential. Superconducting transition-edge sensor detectors can already resolve telecom-wavelength photons of 4 ns duration at a repetition rate of 50 kHz, with an efficiency of 0.88 and negligible noise [28]. In the long run, NbN detectors are promising for achieving higher rates. The detection of 100 ps photons with 100 MHz rate has been reported in ref. [29] with an efficiency of 0.56 and a noise smaller than 10/s.

Our results show the great interest for quantum repeaters of locally generating entangled pairs of excitations with high fidelity. This could also be achieved for physical systems other than atomic ensembles. Promising approaches include the creation of atom-photon entanglement [30] and entangled photon pair sources based on quantum dots [31], which could be combined with quantum memories.

## VI. CONCLUSIONS

We started this work with a quantitative comparison of different quantum repeater protocols using only atomic ensembles and linear optics. This comparison showed that protocols based on the local generation of high-fidelity entangled pairs of atomic excitations make it possible to combine robustness with respect to phase fluctuations and good entanglement distribution rates. We then proposed a new approach for local entanglement generation based on partial memory readout. Together with the use of two-photon detections for long-distance entanglement generation and for entanglement swapping, this approach leads to a repeater protocol that, as far as we know, achieves the highest entanglement distribution rate with the given ingredients. First demonstration experiments should be possible with atomic gases. The protocol could reach its full potential combining fast photon pair sources such as parametric down-conversion and solid-state quantum memories.

We thank R. Dubessy for useful discussions. This work was supported by the EU via the Integrated Project *Qubit Applications (QAP)* and a Marie Curie Excellence

Grant, by the Swiss NCCR *Quantum Photonics*, and by the Chinese National Fundamental Research Program (No. 2006CB921900).

---

[1] H.-J. Briegel, W. Dür, J.I. Cirac, and P. Zoller, Phys. Rev. Lett. **81**, 5932 (1998).

[2] L.-M. Duan, M.D. Lukin, J.I. Cirac, and P. Zoller, Nature **414**, 413 (2001).

[3] C.W. Chou *et al.*, Nature **438**, 828 (2005).

[4] D. Felinto *et al.*, Nature Physics **2**, 844 (2006); Z.-S. Yuan *et al.*, Phys. Rev. Lett. **98**, 180503 (2007); J. Laurat *et al.*, Phys. Rev. Lett. **99**, 180504 (2007); S. Chen *et al.*, Phys. Rev. Lett. **99**, 180505 (2007).

[5] C.W. Chou *et al.*, Science **316**, 1316 (2007).

[6] Y.-A. Chen *et al.*, Nature Physics **4**, 103 (2008).

[7] J. Simon *et al.*, Phys. Rev. Lett. **98**, 183601 (2007).

[8] J. Minář *et al.*, arXiv:0712.0740, to appear in Phys. Rev. A.

[9] L. Jiang, J.M. Taylor, and M.D. Lukin, Phys. Rev. A **76**, 012301 (2007).

[10] Z.-B. Chen *et al.*, Phys. Rev. A **76**, 022329 (2007).

[11] N. Sangouard *et al.*, Phys. Rev. A **76**, 050301(R) (2007).

[12] B. Zhao *et al.*, Phys. Rev. Lett. **98**, 240502 (2007).

[13] J.-W. Pan, C. Simon, C. Brukner, and A. Zeilinger, Nature **410**, 1067 (2001).

[14] D.N. Matsukevich *et al.*, Phys. Rev. Lett. **97**, 013601 (2006); S. Chen *et al.*, Phys. Rev. Lett. **97**, 173004 (2006).

[15] X.-L. Feng *et al.*, Phys. Rev. Lett. **90**, 217902 (2003); L.-M. Duan and H.J. Kimble, Phys. Rev. Lett. **90**, 253601 (2003); C. Simon and W.T.M. Irvine, Phys. Rev. Lett. **91**, 110405 (2003).

[16] The partial readout approach described in Sec. III can be applied to the scheme of Ref. [11], making it possible for one ensemble to serve as single-photon source and memory at the same time.

[17] M. Fleischhauer and M.D. Lukin, Phys. Rev. Lett. **84**, 5094 (2000); T. Chanelière *et al.*, Nature **438**, 833 (2005); M.A. Eisaman *et al.*, *ibid.* **438**, 837 (2005).

[18] Q. Zhang *et al.*, arXiv:quant-ph/0610145.

[19] C. Sliwa and K. Banaszek, Phys. Rev. A **67**, 030101(R) (2003); P. Walther, M. Aspelmeyer, and A. Zeilinger, Phys. Rev. A **75**, 012313 (2007).

[20] C. Simon *et al.*, Phys. Rev. Lett. **98**, 190503 (2007).

[21] N. Gisin, G. Ribordy, W. Tittel, and H. Zbinden, Rev. Mod. Phys. **74**, 145 (2002).

[22] S.A. Moiseev and S. Kröll, Phys. Rev. Lett. **87**, 173601 (2001); M. Nilsson and S. Kröll, Opt. Comm. **247**, 393 (2005); B. Kraus *et al.*, Phys. Rev. A **73**, 020302(R) (2006); A.L. Alexander *et al.*, Phys. Rev. Lett. **96**, 043602 (2006); N. Sangouard *et al.*, Phys. Rev. A. **75**, 032327 (2007).

[23] E. Fraval, M.J. Sellars, and J.J. Longdell, Phys. Rev. Lett. **95**, 030506 (2005).

[24] G. Hétet *et al.*, Phys. Rev. Lett. **100**, 023601 (2008).

[25] O.A. Collins *et al.*, Phys. Rev. Lett. **98**, 060502 (2007).

[26] M.U. Staudt *et al.*, Phys. Rev. Lett. **98**, 113601 (2007); M.U. Staudt *et al.*, Phys. Rev. Lett. **99**, 173602 (2007).

[27] S. Tanzilli *et al.*, Nature **437**, 116 (2005).

[28] D. Rosenberg, A.E. Lita, A.J. Miller and S.W. Nam, Phys. Rev. A **71**, 061803(R) (2005); A.J. Miller, S.W. Nam, J.M. Martinis, and A.V. Sergienko, Appl. Phys. Lett. **83**, 791 (2003).

[29] K.M. Rosfjord *et al.*, Optics Express. **14**, 527 (2006).

[30] B.B. Blinov, D.L. Moehring, L.-M. Duan, and C. Monroe, Nature **428**, 153 (2004); J. Volz *et al.*, Phys. Rev. Lett. **96**, 030404 (2006).

[31] O. Benson, C. Santori, M. Pelton, and Y. Yamamoto, Phys. Rev. Lett. **84**, 2513 (2000); C. Simon and J.P. Poizat, Phys. Rev. Lett. **94**, 030502 (2005); R.M. Stevenson *et al.*, Nature **439**, 179 (2006); N. Akopian *et al.*, Phys. Rev. Lett. **96**, 130501 (2006).